High-sensitivity operation of unshielded radio-frequency atomic magnetometers using phase-lock techniques

Han Yao (姚涵) and Ferruccio Renzoni

Abstract—High sensitivity operation of radio-frequency atomic magnetometers in unshielded environment requires compensation of low-frequency fluctuations of the ambient magnetic field. Here we demonstrate the use of phase-lock techniques to stabilise the magnetic environment and achieve high sensitivity at high frequencies. This is achieved by using the output of the atomic magnetometer both for stabilisation and for measurement purposes. The approach is validated by a proof-of-concept in unshielded environment. The phase-lock approach is also compared to the standard approach where the magnetic environment is stabilised with the help of a set of fluxgate magnetometers, and it is shown that the phase-lock approach features superior performances in signal detection.

Index Terms-atomic magnetometers, quantum sensors

I. INTRODUCTION

TOMIC magnetomers (AMs) [1], [2] have been attracting growing interest due to their extreme sensitivity, low cost, and potential for miniaturization. A wealth of scenarios where atomic magnetometers may play a pivotal role have been explored: from magneto-cardiography (MCG) [3], [4] and magneto-encephalography (MEG) [5] to low-field nuclear magnetic resonance (NMR) [6] and nuclear quadrupole resonance (NQR) detection [7], magnetic nanoparticles detection [8], and electromagnetic induction imaging [9]–[13].

Proof-of-concepts of the extreme sensitivity of atomic magnetometers are typically performed in magnetically controlled environment, with mumetal enclosures used to shield against detrimental ambient noise from DC to frequencies of the order of 100 kHz. This allows to explore the fundamental sensitivity limits. However, real-world applications often require the operations of atomic magnetometers with extreme sensitivity in unshielded environment. This has stimulated the exploration, by different groups, of strategies to be able to retain high sensitivity in the presence of magnetic noise [14]–[18].

In the case of radio-frequency atomic magnetometers (RF-AMs), as covered in this work, the suppression of low-frequency magnetic noise allows for high-sensitivity operation in the RF range [15]. The required stabilisation system can be readily implemented by monitoring the ambient field by using sets of fluxgate magnetometers and compensating for ambient

Corresponding author: Ferruccio Renzoni (email: f.renzoni@ucl.ac.uk). Han Yao is with the School of Physics, Nanjing University of Science and Technology, Nanjing 210094, China. Ferruccio Renzoni is with the Department of Physics and Astronomy, University College London, Gower Street, London WC1E 6BT, UK.

noise with sets of current-carrying coils [14], [15]. In this work we demonstrate an alternative approach for the high sensitivity operation of a radio-frequency atomic magnetometer which does not require additional fluxgate magnetometers to monitor the ambient field. The stabilisation mechanism put forward suppresses low-frequency magnetic field fluctuations. While this obviously does not allow the magnetometer to operate in DC or in low-frequency range, it allows for high-sensitivity operation in the RF range. The approach is validated with experiments in unshielded environment, and a comparison with systems based on fluxgate magnetometers-based stabilisation reveals the superior performance of the approach put forward in this work.

Our approach is ideally suited for applications such as the detection of an RF field of unknown frequency (for e.g., detection of rotating machinery) and for electromagnetic induction imaging. The main advantages are (a) precise in-situ monitoring of the ambient field, and resulting improved sensitivity in unshielded environment; (b) reduced footprint due to the lack of fluxgates, an important aspect for miniaturization and for array operation; (c) extended bandwidth which allows for the detection of signals of unknown frequency.

This work is organised as follows. Section II introduces the concept of the stabilisation system based on phase-locking techniques, with the principles of the established system based on fluxgate magnetometers summarised to readily allow for a comparison. Section III presents a proof-of-concept of the proposed scheme of operation. Section IV analyses the performance of the demonstrated approach, via a detailed sensitivity analysis. Section V examines the enhanced capabilities of test field detection. Conclusions are drawn in Section V.

II. THE PHASE-LOCK MODE: CONCEPT

In this section we introduce our approach to ambient field stabilisation via phase-lock techniques. To this purpose, we first describe the general features of the radio-frequency atomic magnetometer used in this work, to then illustrate the previously used stabilisation system based on sets of fluxgate magnetometers. This will be called the 'fluxgate-lock mode', and will be used to compare the performances of the alternative approach introduced in this work. Finally, the new concept of stabilisation based on phase-lock techniques will be introduced. This will be termed 'the phase-lock mode'.

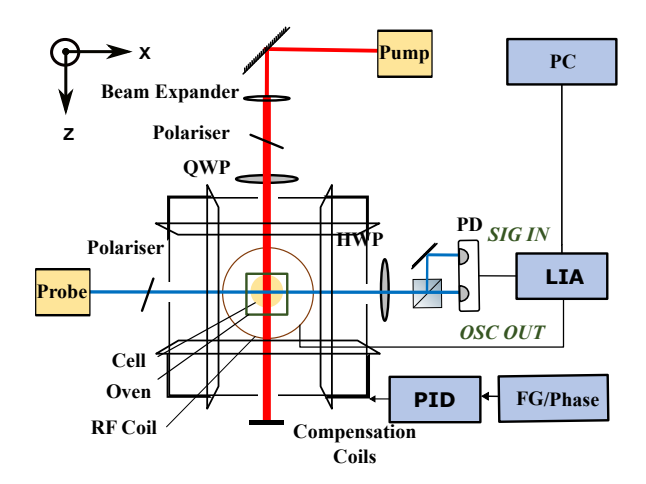


Fig. 1. Arrangement of the double-pump single-probe RF-AM used in this work. The LIA is a Zurich Instruments HF2LI, and its internal oscillator is used to drive the RF coil. Depending on the modality of stabilisation (fluxgate-lock or phase-lock mode), the PID controlling the compensation coils along the z-axis will be fed with an error signal produced by a set of fluxgate magnetometers around the atomic sensor, or by a component of the demodulated polarimeter signal.

A. RF-AM scheme

The core of the RF-AM considered in this work is illustrated in Figure 1 and follows the double-pump single-probe scheme explored in previous work [15]. A pair of circularly polarized counter-propagating pump beams polarize the atomic sample in the presence of a bias magnetic field collinear to the pump axis. The atomic precession is driven by an RF field - also called the *excitation* field in the following - generated by a coil driven by the reference signal of a lock-in amplifier (LIA). The spin precession is read out by a linearly polarized probe beam along the x-axis, whose rotation is monitored by a balanced polarimeter and demodulated by the LIA. The LIA extracts four components: in-phase (absorptive, X), out-of-phase (dispersive, Y), radius $(R = \sqrt{X^2 + Y^2})$ and phase $(\Phi = \tan^{-1}(Y/X))$.

High-sensitivity operation of an RF-AM requires the suppression of ambient noise. The most detrimental component of the ambient noise is the one along the bias magnetic field. Thus, following previous work [15], we will consider a stabilisation scheme where the magnetic noise along the bias field is actively suppressed, so to stabilise the bias field. Helmholtz coils along the two orthogonal components are instead manually adjusted to suppress residual dc fields, without any active stabilisation. The set-up also includes anti-Helmholtz coils along the three orthogonal directions, which are manually adjusted to suppress spurious magnetic field gradients.

B. The fluxgate-lock mode

In the fluxgate-lock (FG) mode, active stabilisation of the bias field is achieved by using one or several fluxgate magnetometers placed in the proximity of the atomic sensor, as illustrated in Figure 2(a). While a single fluxgate has the obvious advantage of simplicity, taking the average of two or more fluxgate magnetometers symmetrically arranged around

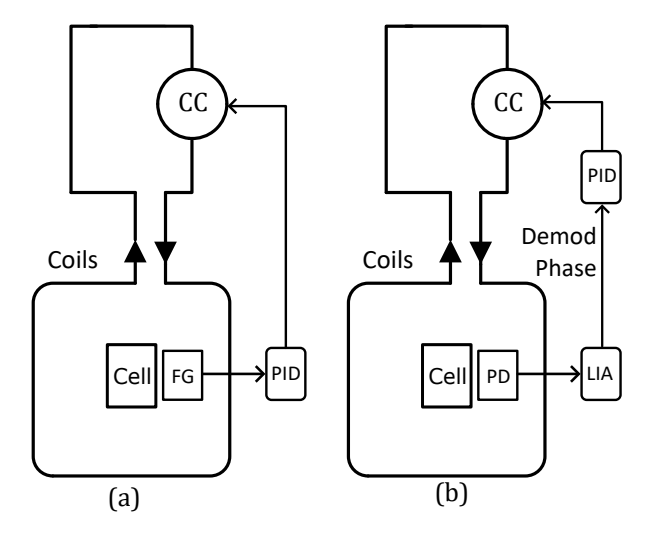


Fig. 2. Sketch of the set-up for the two different active compensation systems considered in this work: (a) the fluxgate-lock mode; (b) the phase-lock mode.

the sensor has the advantage of offering an effectively in-situ measurements of the magnetic field at the center of the cell, and also allows for an increased distance from the atomic magnetometer, reducing the detrimental effect of the residual field generated by the fluxgate magnetometer on the atomic sensor [15]. The error signal generated with the help of the set of fluxgate magnetometers is then used to control the Helmholtz coils in the z-direction and thus provide for the active stabilisation of the bias field.

Stabilisation of the bias field with a bandwidth of 1 kHz allows for high-sensitivity operation of the RF-AM at frequencies larger than the loop cut-off frequency [15].

C. The phase-lock mode

Here, we put forward an alternative approach to the previously introduced fluxgate-lock mode scheme. In our approach, as illustrated in Figure 2(b), the atomic magnetometer readout itself is used as a source signal to stabilise the bias field. Specifically, the phase component of the magnetometer response is used to lock the magnetometer to the magnetic resonance. Ideally, the phase signal should be zero when the RF-AM is at resonance. By feeding the phase to the PID module controlling the bias field, and setting the desired setpoint to zero, the bias field under phase-lock mode is adjusted by the feedback to match the frequency of the precessing atoms and thus the X and R responses are expected to be maintained on the level near resonance. This also holds while the driving frequency is swept over large ranges, hundred kHz or even more: the precessing atoms can sense the change and resonance is maintained.

The phase-lock (PL) mode fundamentally exploits the dispersive feature of atomic magnetic resonance. As illustrated in figure 3, when the RF excitation frequency matches the Larmor frequency (proportional to the bias field), the phase signal crosses zero. This is a critical operating point where the magnetometer exhibits maximum sensitivity to field variations. Any deviation in the bias field shifts the resonance condition, causing a non-zero phase error, as shown in Figure 3. This

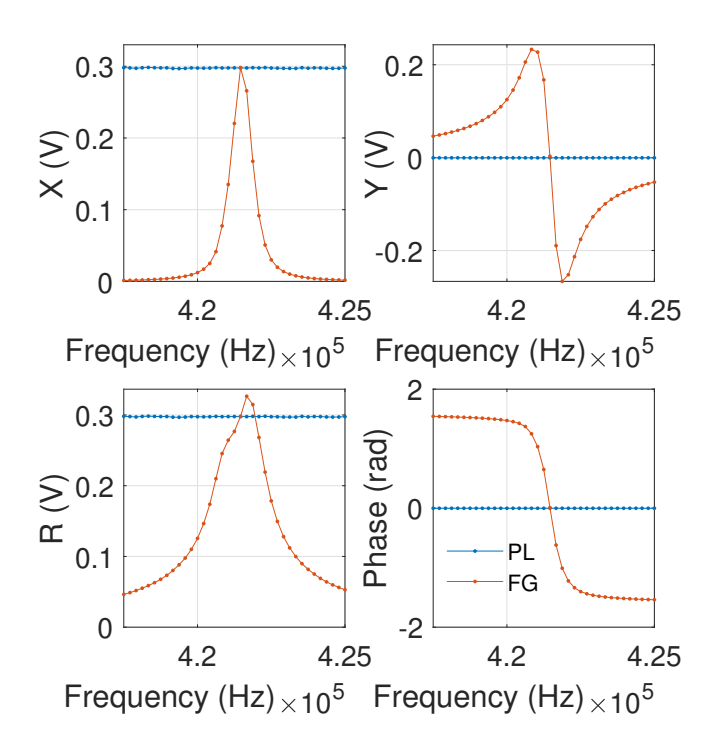


Fig. 3. Comparison of sweeping RF frequency in phase-lock mode and fluxgate-lock mode.

error signal is fed into a PID controller, which dynamically adjusts the compensation current in the z-axis coil to null the phase error. The feedback loop thus locks the system to zero phase, ensuring the continuous maintenance of resonance. Crucially, this self-referencing mechanism eliminates the need for external sensors by directly using the atoms as in-situ field probes. The stability arises because the phase error provides a linear, high-gain correction signal within the loop bandwidth, suppressing low-frequency field noise while enabling widerange frequency sweeps, as it will be demonstrated in the following. This contrasts with the FG mode, where fixed-bias operation restricts bandwidth and sensitivity to off-resonance signals.

Importantly, the PID controller also introduces the separation in frequency required to stabilise the bias field while performing high-frequency measurements. Fluctuations below the PID frequency cut-off are suppressed, while any signal with frequency above the cut-off is left unaffected and can be measured by the atomic magnetometer.

III. EXPERIMENTAL VALIDATION OF THE PHASE-LOCK MODE

A. Experimental parameters of the RF-AM

The phase-lock mode of operation of the RF-AM was validated in unshielded environment using the set-up displayed in Figure 1. All presented experiments were conducted in a complex urban environment, in a densely populated building, in close proximity of a frequently used lift and within hundred meters from underground lines. Operating an atomic magnetometer at high sensitivity in such a continuously changing magnetic environment constitutes a major challenge.

The experimental conditions for the validation, and for all experiments reported in this work, are as follows: 25 mm × 25 mm cell containing isotopically enriched ⁸⁷Rb and 40 Torr nitrogen; cell temperature 85 °C; total pumping light power of two counter-propagation arms of 7.22 mW, for a beam diameter of 13 mm; single-pass probe light of 0.47 mW blue-detuned by about 4 GHz from atomic resonance, with 4mm diameter; RF excitation amplitude of 77 nT. When the system is operated in fluxgate-lock mode, the magnetic field at the centre of the cell is monitored with the help of four fluxgate sensors placed as a square on the same plane of the vapour cell and centered on the cell. The distance between a fluxgate sensor and the cell is 220 mm.

For all measurements, a TTL signal synchronized with the mains electricity supply is generated as a trigger signal and then input into the lock-in amplifier to acquire the magnetometer response of interest, so to mitigate the detrimental effect of the mains interference and raise the signal-to-noise ratio.

B. Phase-lock mode: proof-of-concept

The implementation of the phase-lock mode requires a LIA with two channels which can be operated independently. The two channels of the LIA are used to demodulate the same polarimeter signal when the RF-AM is working in phase-lock mode. The two channels share the phase shift and frequency of the LIA internal oscillator. The output of a fast demodulation channel with a time constant of $T_C=783.2\,$ ns, is fed as input signal to the PID (with cut-off frequency 7 kHz) which controls the current into the z-direction coil while the output of the other channel, with a time constant of $T_C=10.16\,$ ms, constitutes our measurement. The value of T_C for the measurement channel is the same as the one used in FG mode, so to allow for a direct comparison of the results. Figure 4 shows the phase of two channels recorded over the duration of 10 s with the stabilisation loop left open.

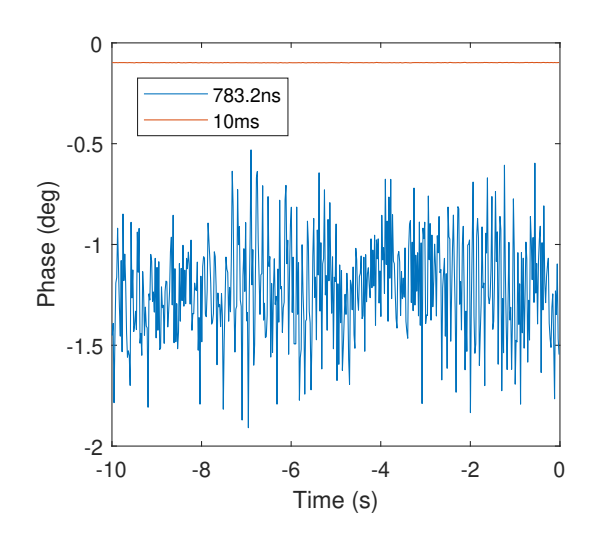


Fig. 4. 10 s records of the phase of two demodulation channels of different time constant

Before closing the feedback loop in phase-lock mode, the phase shift of the lock-in internal oscillator with respect to the phase of the polarimeter signal is adjusted, so to set to zero the offset of the phase of the measurement channel. When the phase of the magnetometer is locked to resonance, the phase response of the measurement channel is expected to display small fluctuations around zero.

Results for the operation of the RF-AM in phase-lock mode are reported in Figure 3. Separate experiments for the fluxgate-lock mode were also conducted, with results reported in the same figure for comparison purposes.

In the experiments, the bias field is initially set to the value corresponding to the desired resonant frequency, effectively tuning the magnetometer. Then the RF field frequency is swept around the resonance frequency, for both cases of fluxgate-lock mode and phase-lock mode separately.

In case of the fluxgate lock-mode, the feedback maintains the bias field to the initially set value, and we recover the familiar (dispersive, for the Y and Phase) Lorentzian atomic resonance in all four output channels of the LIA. Instead, in the case of phase-lock mode, the fast phase channel of the LIA is used to lock the AM to zero-phase, i.e. to the maximum of the atomic resonance. The bias field thus follows the sweeping RF field. In this mode, the slow outputs of the LIA, i.e. the four measurement channels, have values corresponding to the peak of the atomic resonance. The values of the measurement channels do not vary while sweeping the RF frequency as the AM is locked to the peak of the resonance.

A first qualitative estimate of the performance in the phase-lock mode is obtained by monitoring the stability of the AM over time, and evaluating the noise level in the frequency domain. Figure 5 compares the stability of the RF-AM at resonance in the three different configuration of relevance here: the open loop, the fluxgate-lock mode and phase-lock mode. The time traces recorded over ten seconds of the AM outputs in the different configuration clearly reveal the superior stability of the AM in phase-lock mode.

Figure 6 compares the signal amplitude spectrum measured under fluxgate-lock mode and phase-lock mode, separately, with the open-loop spectrum also reported for comparison. The peaks observed at resonance (i.e., zero detuning) for the fluxgate-lock mode and for the phase-lock mode are of comparable amplitude, and significantly larger than the one observed in open loop. The baseline noise for the phase-lock mode is lower than that for the case of the fluxgate-lock mode, thus again confirming qualitatively the better performance of the RF-AM in phase-lock mode.

IV. SENSITIVITY ANALYSIS

A quantitative assessment of the performance of the RF-AM in phase-lock mode requires the measurement of the sensitivity. The sensitivity of the RF-AM in fluxgate-lock mode will also be determined, for comparison.

Under fluxgate-lock mode, the sensitivity analysis was carried out following standard procedure [15]. Both DC and AC sensitivities are considered here. The DC sensitivity δB_{DC} refers to the smallest detectable shift of the bias field. It is considered here to be consistent with standard characterization of magnetometers, but we stress that the proposed system is

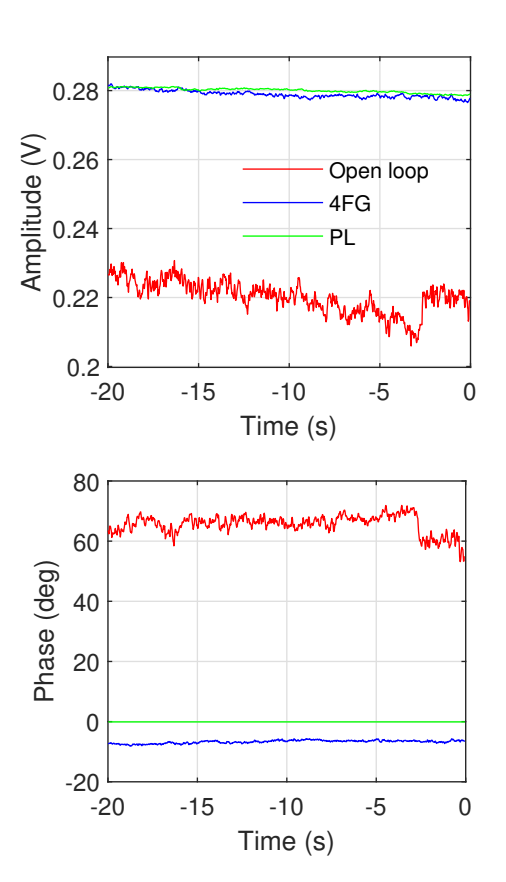


Fig. 5. Comparison of the phase stability of the AM in three different configurations: open loop, phase-lock mode and fluxgate-lock mode. All phase signals were taken from the demodulation channel of the LIA with a time constant of 10.16 ms. The different offsets are due to the inaccuracy in the determination of the resonance frequency from a fit of the atomic resonance. In detail, the excitation frequency is set manually for the presented measurements. Operation in the phase-lock mode forces the atomic resonance frequency to track the excitation frequency by adjusting the bias field, so that exact resonance is achieved. Instead, in the fluxgate-lock mode or in open loop mode, the resonance frequency is determined from a fit of the atomic resonance, and then the excitation frequency is adjusted manually to match the atomic resonance frequency. As a result of this approach, the frequency and according the phase may be slightly detuned from resonance.

not designed to be used for DC field measurements. This is because the stabilisation of the bias field leads to an automatic compensation of any additional static field, hence altering it. The DC sensitivity is given by

$$\delta B_{DC} = \frac{\hbar}{g_F \mu_B} \frac{\Gamma}{\sqrt{RBW}SNR} , \qquad (1)$$

where μ_B is the Bohr magneton, g_F is the Landé factor, \hbar is the reduced Planck's constant, RBW is the resolution bandwidth and Γ is the full width at half maximum (FWHM) of the magnetic resonance. The SNR is measured as the square root of the ratio between the maximum value of the power spectrum density (PSD) with the RF field on and the mean value of the noise power spectrum density with the RF field turned off, which is also referred to as the noise floor.

The AC sensitivity (AC) refers to the ability to detect AC fields, and is given by

$$\delta B_{AC} = \frac{B_{RF}}{\sqrt{RBW}SNR} \tag{2}$$

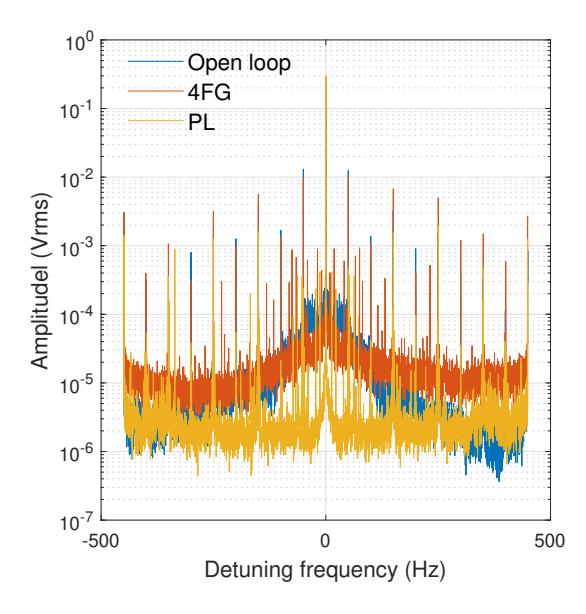


Fig. 6. Comparison of signal amplitude spectrum in open loop, phase-lock mode and fluxgate-lock mode. The horizontal axis represents the frequency detuning from resonance (415.746 kHz).

where B_{RF} is the RF field applied for calibration purposes. We stress here that the AC sensitivity has a true operational meaning. The stabilisation mechanism only suppresses low-frequency flucuations, and in particular stabilises the bias field. For frequencies beyond the bandwidth of the stabilisation loop, true measurements of RF fields can be performed.

The DC sensitivity was measured to be 13 fT/Hz^{1/2} and the AC sensitivity was determined to be 47 fT/Hz^{1/2} at 415.746 kHz. However we note that the same approach for the determination of sensitivity cannot be directly applied to the RF-AM operating in phase-lock mode. Indeed, in the standard approach [15], both AC and DC sensitivities are calculated from the signal-to-noise ratio (SNR). The measurements thus involve turning off the RF field to evaluate the noise spectrum. However, this is not applicable to the RF-AM in phase-lock mode as the phase cannot stay locked with the RF field off. To evaluate the performance of phase-lock mode and to make a comparison with the fluxgate-lock mode, we will thus follow an alternative approach.

Inspired by Ref. [19], we measured both the signal amplitude spectrum (AS) and the signal amplitude spectral density (ASD) with the RF field on and took the value of the detuned signal amplitude spectral density (ASD') as the noise level, as reported in table I. The signal level was measured in a standard way, i.e., as the peak of the signal amplitude spectrum. The two quantities were then combined to form a measure of the signal-to-noise ratio. Such a measure will be indicated by SNR' to distinguish it from the signal-to-noise ratio SNR obtained by turning off the RF. The signal to noise ratio and sensitivities were then determined following standard procedure [15], but using SNR' instead of SNR. The spectra used in the determination of the sensitivity are reported in Figure 7. Comparisons were made in Table I between SNR and SNR' and between the fluxgate-lock mode and phase-lock

TABLE I SNR and SNR $^\prime$ of the fluxgate-lock mode and phase-lock mode.

	4FG	PL
Signal (Vrms)	3.08E-01	3.00E-01
SNR	1.21E+06	NA
ASD $(T/Hz^{1/2})$	4.52E-14	NA
SNR'	9.21E+05	1.19E+06
ASD' $(T/Hz^{1/2})$	5.93E-14	4.59E-14

mode.

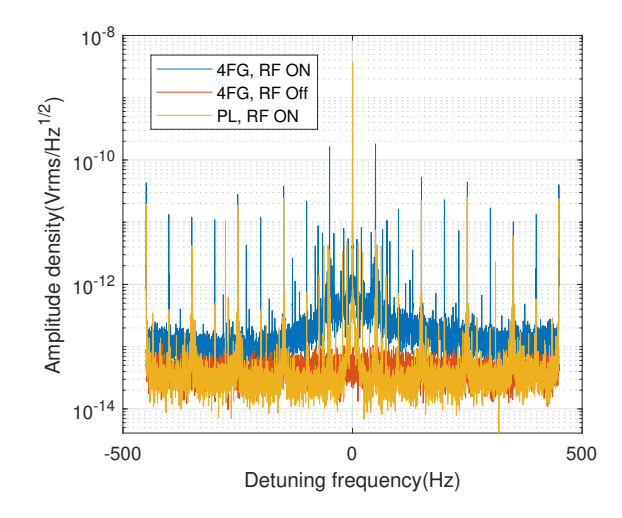


Fig. 7. Amplitude spectrum density in open loop, fluxgate-lock mode and phase-lock mode. The horizontal axis represents the frequency detuning from resonance (415.746 kHz).

V. TEST FIELD DETECTION

The performances of the RF-AM in phase-lock mode can be further evaluated by assessing the ability to detect an applied oscillating magnetic field. A direct comparison with the performances of the RF-AM in fluxgate-locked mode will also be carried out.

A test field is applied on the magnetometer in the presence of the excitation field which drives the RF-AM. The test coil and the excitation coil are identical, 20 cm in diameter, 2 turns. One is placed above the cell at a distance of 10 cm while the other is 10 cm below the cell. In our tests, the frequency of the field driving the magnetometer is swept around the atomic resonance frequency, for a fixed value of the bias field and given frequency and amplitude of the test field.

We examine first the performance of the RF-AM in fluxgate-locked mode. Our results for the magnetometer's response under the fluxgate-lock mode are reported in Figure 8, for a test field frequency of 415 kHz. The response to test field amplitudes of 10%, 20% and 30% of the excitation field was evaluated. Our results indicate that the 10% test field can barely be resolved. Only by subtracting the background response measured with the test field off can the test field with

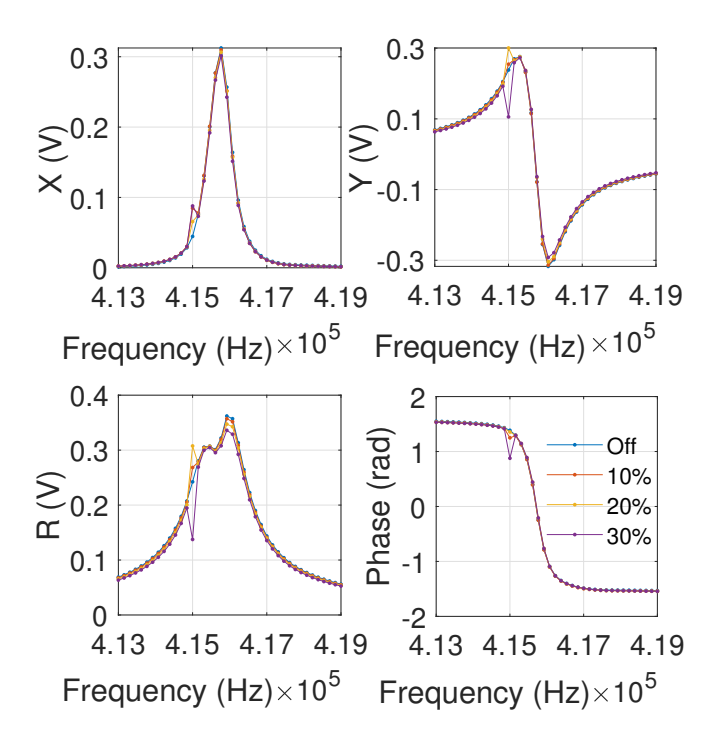


Fig. 8. Detection of a test field with the RF-AM in fluxgate-lock mode. The XYRP components of the RF-AM response are reported for different values of the amplitude of the test field, indicated in the figure as a fraction of the amplitude of the excitation field. The frequency of the test field is 415 kHz, and the amplitude of the excitation field is 77 nT.

the smallest amplitude considered (10% of the excitation field) be clearly resolved, as shown in Figure 9.

We consider now the response of the RF-AM in phase-lock mode. Our results of Figure 10 show that the RF-AM in phase-lock mode exhibits a stronger response than in fluxgate-lock mode under the same conditions: the test field of amplitudes 10%, 20% and 30% of the excitation field is clearly resolved in all four components XYRP of the magnetometer response.

Given the stronger response observed in the phase-lock mode, we performed further tests in such a configuration for lower test field amplitudes, with results reported in Figure 11. These results report the successful detection of fields with amplitude of 1% the amplitude of the excitation field. This is a quantitative proof of the superior performance of the RF-AM in phase-lock mode with respect to the fluxgate-lock mode.

The capability to detect a test field was further explored by taking additional series of measurements for different frequencies of the test field. For all these measurements, the resonance frequency of the magnetometer is set at 415.746 kHz. Measurements were performed both in phase-lock mode and in fluxgate-lock mode, so to compare the detection capabilities of our new approach with the standard one. Results for the fluxgate-lock mode are reported in Figure 12 while the data in Figure 13 is taken under phase-lock mode. In both mode of operation, the RF-AM shows a stronger response to the test field frequency of 415 kHz. The reported data also show clear evidence that the response to the test field of varying frequencies is more uniform under phase-lock mode,

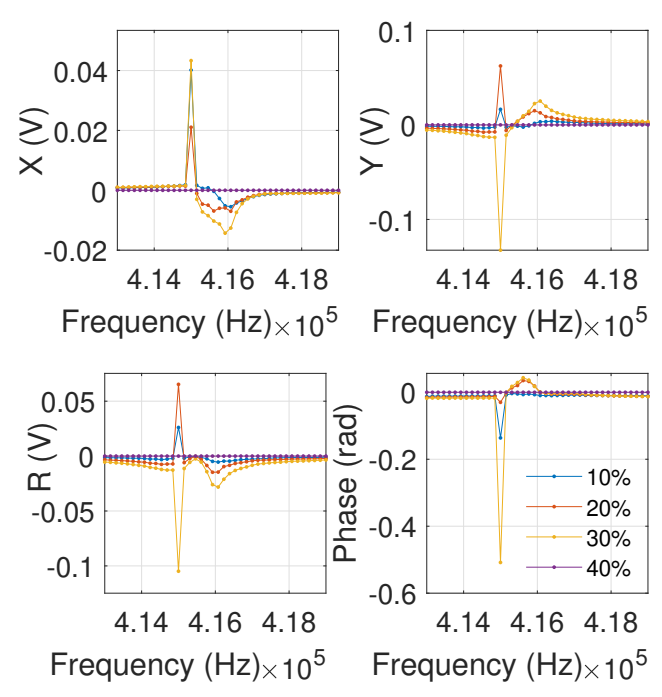


Fig. 9. Detection of a test field with the RF-AM in fluxgate-lock mode with background subtraction. The XYRP components of the RF-AM response are reported for different values of the amplitude of the test field, indicated in the figure as a fraction of the amplitude of the excitation field. The response with the test field off is subtracted from all reported data sets. The frequency of the test field is 415 kHz, and the amplitude of the excitation field is 77 nT.

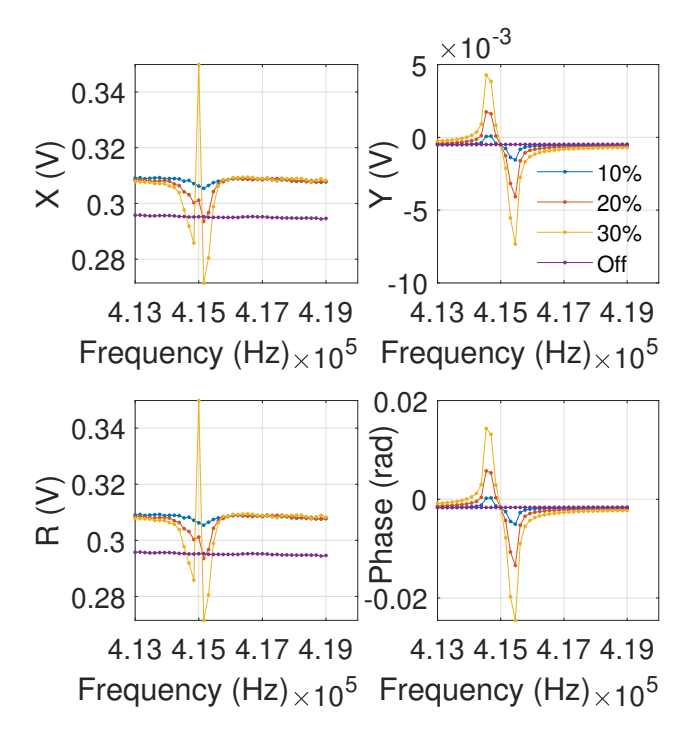


Fig. 10. Detection of a test field with the RF-AM in phase-lock mode: The XYRP components of the RF-AM response are reported for different values of the amplitude of the test field, indicated in the figure as a fraction of the amplitude of the excitation field. The frequency of the test field is 415 kHz, and the amplitude of the excitation field is 77 nT.

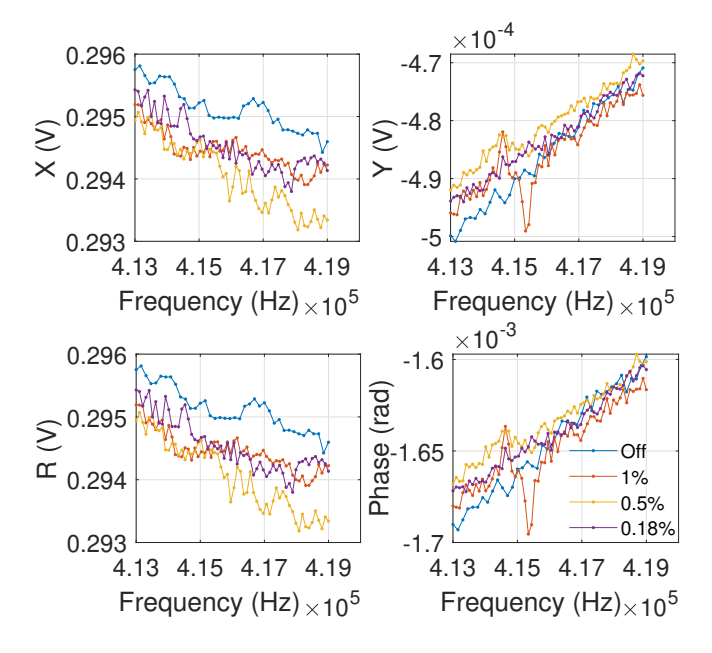


Fig. 11. Detection of a test field with the RF-AM in phase-lock mode. The response of the RF-AM to test field amplitudes test field is 1%, 0.5% and 0.18% of the excitation field of 77 nT. The frequency of the test field is 415 kHz.

especially in the Y and Phi components. This is because the phase-lock mode enables the magnetometer to remain on resonance while the frequency is changed. Operation of the RF-AM in phase-lock mode also allows for the clear identification of the frequency of the test field. In the case of the fluxgate-lock mode, we also investigated the potential improvement produced by the subtraction of the background. Results of the background subtraction from the data of Figure 12 are reported in Figure 14. The procedure fails to improve the resolution of the test field frequencies and also the response of the atomic magnetometer is significantly less uniform than under phase-lock mode.

The superior performance of the operation in phase-lock mode is even more evident when considering the detection of a signal of unknown frequency. We note that the bandwidth under fluxgate-locked mode is typically below 1 kHz, and specifically for the present work the FWHM is around 700 Hz. Thus, for a fixed bias field, one can detect signal over a range of 1 kHz, by also performing background subtraction as to enhance detection capabilities. To explore a wider range of frequencies, one needs to re-tune the RF-AM by changing the bias field, and performing background subtraction at each retuning. It is obviously impractical to subtract the background once every bandwidth, particularly when the target frequency is not known and thus the scan range is large. Operation in phase-lock mode overcomes such a limitation. Our results in phase-lock mode presented in Figure 15 show that the phase can stay locked for an RF frequency sweeping range as wide as 60 kHz, with the maximum range being determined by the range of the PID feedback. Also, Figure 15 evidences a significantly flat response over the considered range, with the minimum of the R response over the range being 96% of the maximum. Thus, the phase-lock exhibits a significantly

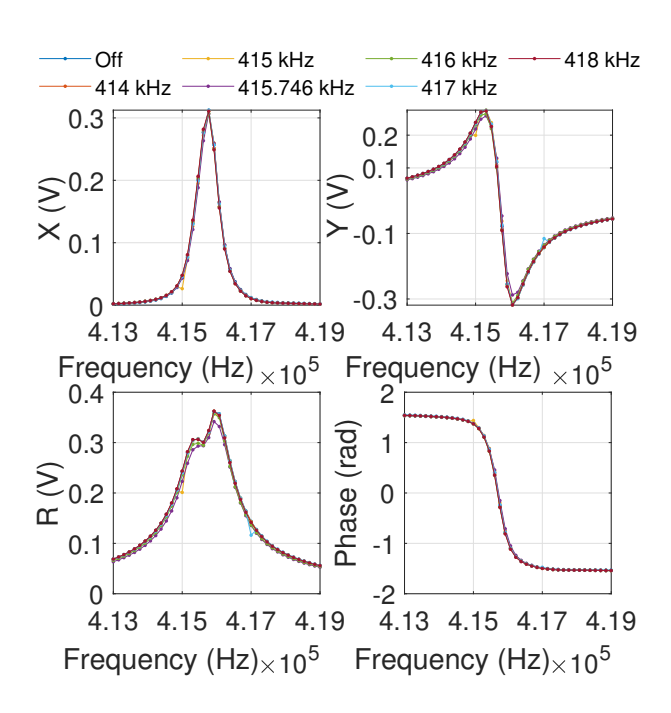


Fig. 12. Detection of a test field of variable frequency with the RF-AM in fluxgate-lock mode. The XYRP response is reported for different frequencies of the test field, for a fixed test field amplitude of 7.7 nT.

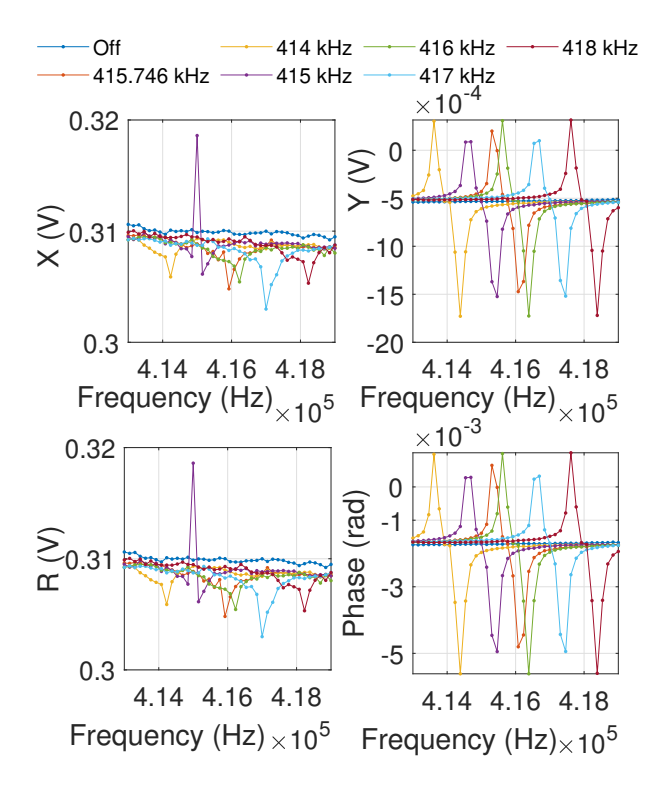


Fig. 13. Detection of a test field of variable frequency with the RF-AM in phase-lock mode. The XYRP response is reported for different frequencies of the test field, for a fixed test field amplitude of 7.7 nT.

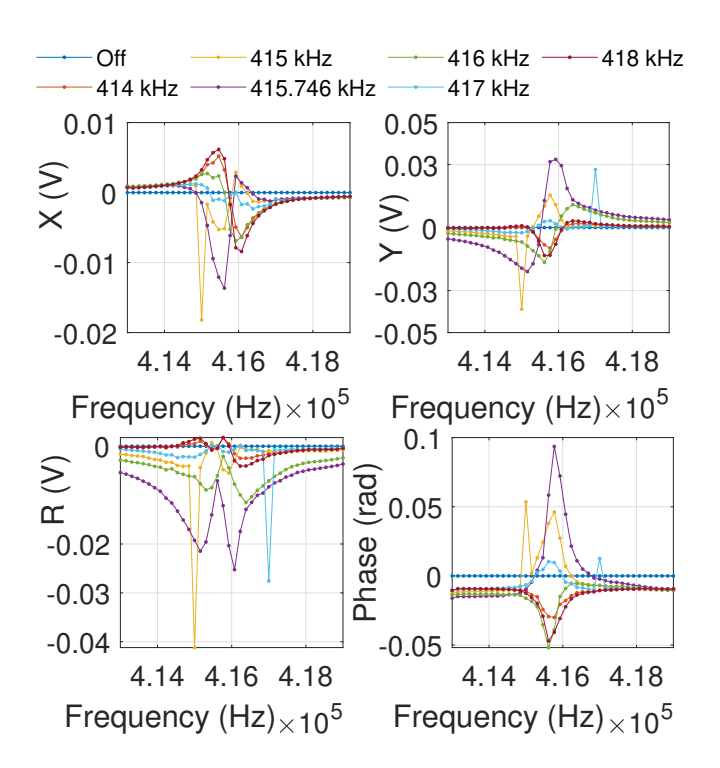


Fig. 14. Detection of a test field of variable frequency with the RF-AM in fluxgate-lock mode and background subtraction. The XYRP response is reported for different frequencies of the test field, for a fixed test field amplitude of 7.7 nT. The data is obtained by subtracting from each data set of Figure 12 the response with test field off.

larger bandwidth than under the fluxgate-lock mode, with a flat response. This satisfies the requirement for detection of signals of unknown frequency, with immediate applications including the detection and identification of rotating machinery (e.g., drones).

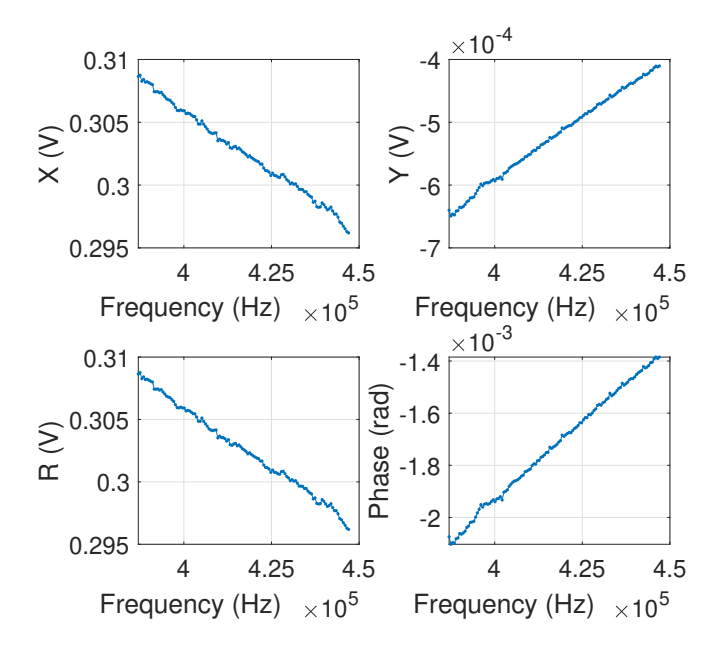


Fig. 15. Sweeping RF frequency from 387 to 477 kHz under phase-lock mode

Previous work in FG mode [20] revealed that in unshielded

environment operating the atomic magnetometer slightly detuned from resonance improves the detection capabilities. In fact, while in an ideal noise-free environment operating on exact resonance makes the AM most sensitive to a test field, in the presence of magnetic noise a frequency offset decreases the detrimental role of the bias field fluctuations, offsetting the decrease in absolute sensitivity of the magnetometer. This results in an overall stronger response to a test field [20]. In the present context of the PL mode, we explore whether similar reasoning applies, with a phase offset improving test field detection. To this purpose, the effect of a finite offset in the phase offset point was investigated. The performance of signal detection capability of the RF-AM in phase-lock mode is indeed found further improved by adding an offset to the phase locking point. Figure 16 shows the responses of the RF-AM in phase-lock mode to a test field for different values of the offset. The phase response under fluxgate-mode without test field is also reported for a more straightforward visualisation of the connection between the phases and the detunings.

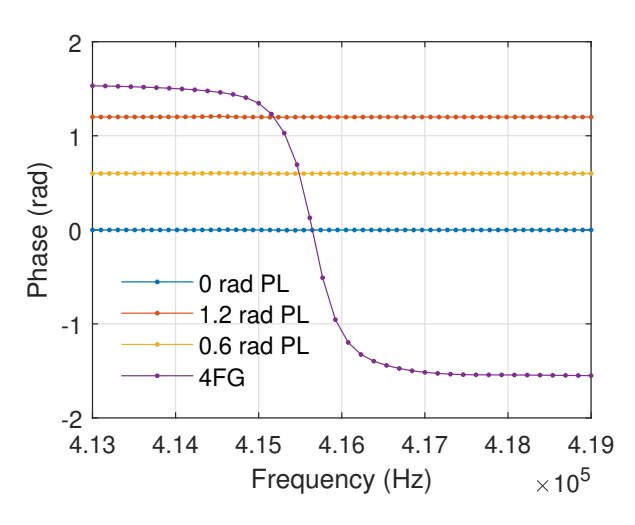


Fig. 16. Phase response of the RF-AM in phase-lock mode to a test field, with the locking point set at a finite offset from zero. Different data sets corresponds to different values of the offset. The response for the RF-AM in fluxgate-lock mode without test field is also reported for an immediate visualisation of the connection between frequency detuning and phase. The test field is fixed at 7.7 nT and 415 kHz.

For a better visualisation of the results, the average offset in the phase response is removed from each data set, so that the data can be displayed on a larger scale, as shown in Figure 17. A strong response to the test field is evidenced, and it appears that the response in both amplitude and phase is significantly increased for larger phase offset, i.e. the signal detection capability is enhanced by a finite offset in the phase locking point.

A quantitative measure of the enhancement in signal detection can be obtained by calculating for each data set the maximum deviation ΔR and ΔP from the average, with results reported in Figure 18 for different values of the locking point.

These results quantifies the enhancement in signal detection: the more detuned from 0 rad the phase locking point is,

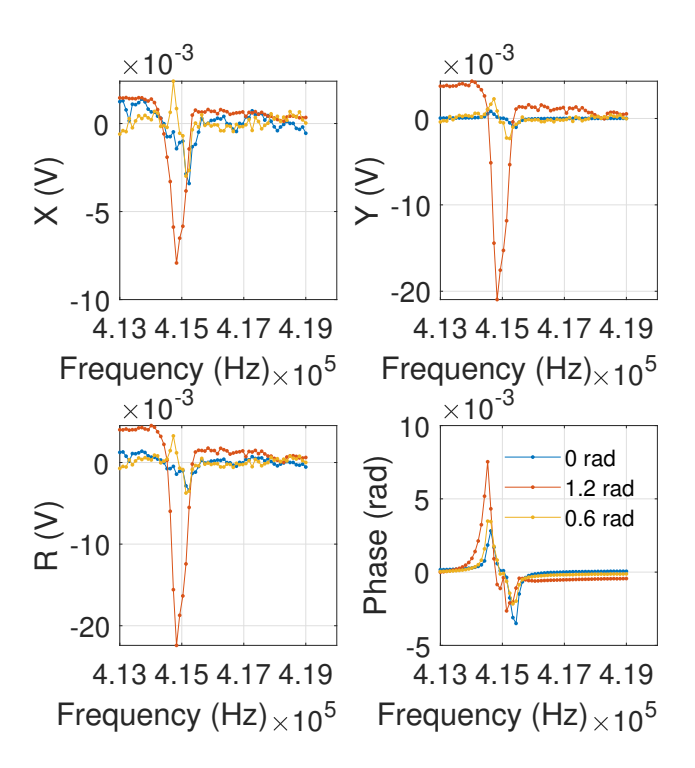


Fig. 17. Detection of a test field with the RF-AM in phase-lock mode, with a finite offset introduced in the phase locking point. The XYRP responses under the phase-lock mode is plotted as a function of the frequency for different values of the phase locking point. The test field amplitude is fixed at 7.7 nT and the frequency at 415 kHz.

the larger the deviations caused by the test field in both the amplitude and phase components.

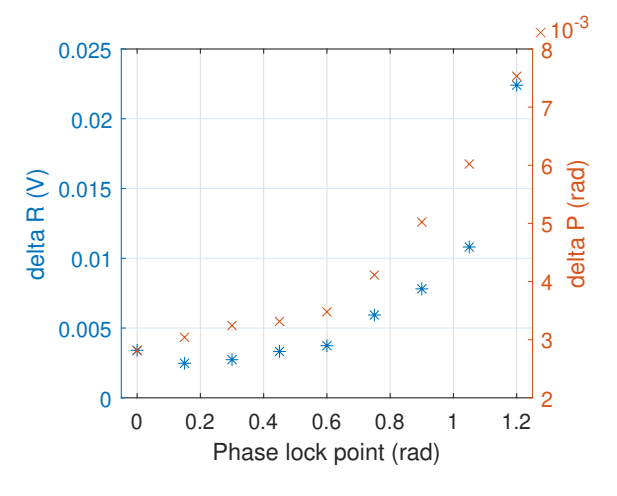


Fig. 18. Enhancement in signal detection of the RF-AM in phase-lock mode, as produced by a finite value of the phase lock point. The deviations in amplitude and phase signal response caused by the test field are plotted for different values of the locking point. The test field amplitude is fixed at 7.7 nT and the frequency at 415 kHz.

VI. CONCLUSIONS

This work addressed the issue of stabilisation of the magnetic environment so to allow high-sensitivity operation of atomic magnetometers in unshielded settings. We put forward a new mode of operation, termed the phase-lock mode, of a

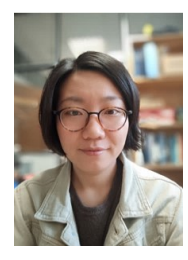
radio-frequency atomic magnetometer which relies on the fast demodulation of the phase measurement of the magnetometer as a real-time in-situ measurement of the field fluctuations on the sensor. We presented a detailed evaluation of the approach, and compared it with the standard set-up based on monitoring the background field with the help of a set of fluxgate magnetometers. Operation in phase-lock mode exhibits superior performances with respect to the standard mode of operation. In fact, regardless of the number of fluxgates employed in the FG mode, the PL mode offers several advantages. First, the lack of fluxgates allows for miniaturization and array operation. Second, the sensitivity of fluxgates is significantly worse than the one of an atomic magnetometer, hence the phase-lock mode leads to a better stabilisation of the bias field and hence to a higher sensitivity of the atomic magnetometer. Third, the bandwidth of the PL-mode is far superior to the FG-mode.

The PL mode of operation demonstrated in this work is very well suited to signal detection, and we forecast immediate applications in electromagnetically induction imaging.

REFERENCES

- [1] D. Budker and M. Romalis, "Optical magnetometry," *Nature Physics*, vol. 3, no. 4, pp. 227–234, 2007.
- [2] A. Fabricant, I. Novikova, and G. Bison, "How to build a magnetometer with thermal atomic vapor: a tutorial," *New Journal* of *Physics*, vol. 25, no. 2, p. 025001, feb 2023. [Online]. Available: https://dx.doi.org/10.1088/1367-2630/acb840
- [3] G. Bison, R. Wynands, and A. Weis, "Dynamical mapping of the human cardiomagnetic field with a room-temperature, laser-optical sensor," *Optics Express*, vol. 11, no. 8, pp. 904–909, 2003.
- [4] Y. Yang, M. Xu, A. Liang, Y. Yin, X. Ma, Y. Gao, and X. Ning, "A new wearable multichannel magnetocardiogram system with a SERF atomic magnetometer array," *Scientific Reports*, vol. 11, no. 1, pp. 1–11, 2021.
- [5] E. Boto, N. Holmes, J. Leggett, G. Roberts, V. Shah, S. S. Meyer, L. D. Muñoz, K. J. Mullinger, T. M. Tierney, S. Bestmann *et al.*, "Moving magnetoencephalography towards real-world applications with a wearable system," *Nature*, vol. 555, no. 7698, pp. 657–661, 2018.
- [6] M. Ledbetter, I. Savukov, D. Budker, V. Shah, S. Knappe, J. Kitching, D. Michalak, S. Xu, and A. Pines, "Zero-field remote detection of NMR with a microfabricated atomic magnetometer," *Proceedings of the National Academy of Sciences*, vol. 105, no. 7, pp. 2286–2290, 2008.
- [7] S.-K. Lee, K. Sauer, S. Seltzer, O. Alem, and M. Romalis, "Subfemtotesla radio-frequency atomic magnetometer for detection of nuclear quadrupole resonance," *Applied Physics Letters*, vol. 89, no. 21, p. 214106, 2006.
- [8] X. He, Y. Ma, Y. Chen, Z. Xu, Y. Li, L. Wu, Y. Ruan, W. Zheng, K. Li, and Q. Lin, "Precise detection of trace magnetic nanoparticles based on spin-exchange-relaxation-free magnetometers," *Applied Physics Letters*, vol. 125, no. 7, p. 073702, 08 2024. [Online]. Available: https://doi.org/10.1063/5.0212803
- [9] A. Wickenbrock, S. Jurgilas, A. Dow, L. Marmugi, and F. Renzoni, "Magnetic induction tomography using an all-optical 87rb atomic magnetometer," *Optics Letters*, vol. 39, no. 22, pp. 6367–6370, Nov 2014. [Online]. Available: http://opg.optica.org/ol/abstract.cfm?URI= ol-39-22-6367
- [10] C. Deans, L. Marmugi, S. Hussain, and F. Renzoni, "Electromagnetic induction imaging with a radio-frequency atomic magnetometer," *Applied Physics Letters*, vol. 108, no. 10, p. 103503, 2016.
- [11] P. Bevington, R. Gartman, W. Chalupczak, C. Deans, L. Marmugi, and F. Renzoni, "Non-destructive structural imaging of steelwork with atomic magnetometers," *Applied Physics Letters*, vol. 113, no. 6, p. 063503, 2018.
- [12] K. Jensen, M. Zugenmaier, J. Arnbak, H. Stærkind, M. V. Balabas, and E. S. Polzik, "Detection of low-conductivity objects using eddy current measurements with an optical magnetometer," *Physical Review Research*, vol. 1, no. 3, p. 033087, 2019.
- [13] F. Fang and Z. Wang, "Electromagnetic induction imaging with a serf atomic magnetometer," *Optics Laser Technology*, vol. 182, p. 112144, 2025

- [14] C. Deans, L. Marmugi, and F. Renzoni, "Sub-picotesla widely tunable atomic magnetometer operating at room-temperature in unshielded environments," *Review of Scientific Instruments*, vol. 89, no. 8, p. 083111, 2018
- [15] H. Yao, B. Maddox, and F. Renzoni, "High-sensitivity operation of an unshielded single cell radio-frequency atomic magnetometer," *Optics Express*, vol. 30, no. 23, pp. 42015–42025, Nov 2022. [Online]. Available: https://opg.optica.org/oe/abstract.cfm?URI=oe-30-23-42015
- [16] J. E. Dhombridge, N. R. Claussen, J. Livanainen, and P. Schwindt, "High-sensitivity rf detection using an optically pumped comagnetometer based on natural-abundance rubidium with active ambient-field cancellation," *Physics Review Applied*, vol. 18, p. 044052, 2022.
- [17] H. Yao, B. Maddox, and F. Renzoni, "Neural network-aided optimisation of a radio-frequency atomic magnetometer," *Opt. Express*, vol. 31, no. 17, pp. 27287–27295, 2023. [Online]. Available: https://opg.optica.org/oe/abstract.cfm?URI=oe-31-17-27287
- [18] B. Maddox and F. Renzoni, "Two-photon electromagnetic induction imaging with an atomic magnetometer," *Applied Physics Letters*, vol. 122, no. 14, p. 144001, 04 2023.
- [19] R. Zhang, R. Mhaskar, K. Smith, and M. Prouty, "Portable intrinsic gradiometer for ultra-sensitive detection of magnetic gradient in unshielded environment," *Applied Physics Letters*, vol. 116, no. 14, p. 143501, 04 2020.
- [20] L. Marmugi, C. Deans, and F. Renzoni, "Electromagnetic induction imaging with atomic magnetometers: Unlocking the low-conductivity regime," *Applied Physics Letters*, vol. 115, no. 8, p. 083503, 2019.



Han Yao received her B.E. degree in measurement and instrumentation from Beihang University, Beijing, China, in 2015. In 2024 she received her PhD in Physics from University College London (UCL), London (UK). After a post-doctoral position at UCL, to October 2024 she was appointed to an Associate Professor position at the School of Physics, Nanjing University of Science and Technology, Nanjing 210094, China.



Ferruccio Renzoni received the M.Sc. degree in physics from the University of Pisa (Italy) in 1993, the Ph.D. degree from the Technische Universitaet Graz (Austria) in 1998, and in 2003 the Habilitation à diriger des recherches from Ecole Normale Superieure, Paris, France. In October 2003, he joined University College London (U.K.) as a Lecturer, to be then promoted to a Reader and a Professor.